

## SHORT-RANGE PREDICTION OF BANDED PRECIPITATION ASSOCIATED WITH DEFORMATION AND FRONTOGENETIC FORCING

Peter C. Banacos\*  
NOAA/NWS/NCEP/Storm Prediction Center  
Norman, Oklahoma 73069

### 1. INTRODUCTION

It is common from a radar vantage point to observe narrowly banded reflectivity structures having a length-to-width ratio on the frontal scale (5-50 km in width and 100-1000 km in length). The importance of these mesoscale bands lies in their potential to produce highly localized heavy precipitation. During the cold season, snowfall rates in excess of 1"/hr are frequently observed, with up to 5"/hr in extreme cases. Less frequent warm season events can produce locally heavy rainfall in excess of 2"/hr resulting in the potential for flash floods. The spatial location and duration of these areas is often difficult to predict accurately. In addition, differentiating between large-scale precipitation events exhibiting little mesoscale variance, and those exhibiting highly organized mesoscale banding, is an important operational forecast problem that is not always well forecast by the suite of operational numerical models. The goal of this paper is to describe a "mode" of banded precipitation that occurs with a distinct col point in the horizontal flow aloft. An emphasis is placed on observational aspects of these events, which may aid in forecasting their timing and location, particularly in the short-range forecast period (0-12 h).

### 2. SYNOPTIC SETTING

The synoptic-scale setting favorable for the development of mesoscale banding is usually characterized by horizontal deformation in the 850-500 mb layer, with the deformation zone often most pronounced near 700 mb. From a pattern-recognition standpoint, it is convenient to place large-scale deformation zones into two categories: (1) those occurring in conjunction with strong extratropical cyclogenesis (Fig. 1a), and (2) those associated with strong east-west oriented frontal zones with modest or minimal surface cyclone development (Fig. 1b). In the former case, the deformation develops as the cyclone deepens from an open wave to a closed low in the middle-troposphere. A diffluent flow region develops in the northwest quadrant of the cyclone, sometimes west of a surface inverted trough, where the low-level cold conveyor belt (CCB) splits. A portion of the flow turns counterclockwise around the low-level circulation while the other branch turns clockwise to become part of poleward flow in advance of the upstream shortwave trough (Schultz 2001). Banding associated with strong cyclones is common in the Northeast U.S. during winter.

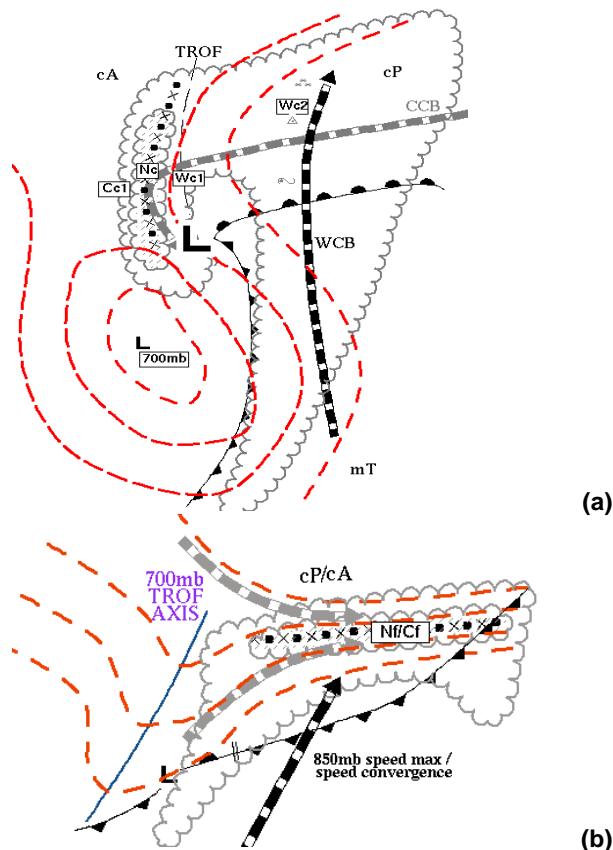


**Fig. 1** Schematic deformation zones (denoted by axes of filled circles and x's) occurring in association with (a) rapid cyclogenesis and (b) frontal zones with modest surface cyclone development. Dashed lines represent 700 mb height. Scalloped region denotes high-level cloud pattern. Other symbols are described in the text.

In the frontal/weak cyclogenesis pattern, the 700 mb flow is often characterized by a positive tilt trough and downstream confluent flow several hundred kilometers to the north of a polar or arctic front. A weak low center is usually found along the surface boundary, with mesoscale banding occurring to the north and/or northeast of the cyclone. In cases of very strong low-level static stability, a surface low may not exist, making the situational awareness of the forecaster to heavy precipitation potential generally lower than in the strong cyclogenesis case.

Deformation in the latter case is achieved through confluent 700 mb flow parallel to the baroclinic zone. Speed convergence at the nose of a southerly low-level jet, which increases the horizontal temperature gradient on its poleward edge, may also be present. The frontal/weak cyclogenesis pattern is common in continental areas, particularly the Great Plains and Great Lakes regions during the winter.

\* Corresponding author address: Peter C. Banacos, Storm Prediction Center, 1313 Halley Circle, Norman, OK 73069; e-mail: peter.banacos@noaa.gov

### 3. PHYSICAL CONSIDERATIONS

The utility of identifying horizontal deformation for the purpose of mesoscale banding potential stems from its first-order contribution to the two-dimensional frontogenesis function, defined as (Petterssen 1940):

$$F = \frac{D}{Dt} |\nabla_p \mathbf{q}| \quad (1)$$

where  $F$  is the scalar, two-dimensional form of frontogenesis,  $\nabla_p \mathbf{q}$  is the quasi-horizontal gradient of potential temperature, and  $D/Dt$  is the total derivative following air parcel motion. The relationship between  $F$  and deformation can be shown more explicitly using an alternate form of the equation (Petterssen 1936):

$$\frac{D}{Dt} |\nabla_p \mathbf{q}| = -\frac{1}{2} |\nabla_p \mathbf{q}| (D - E \cos 2b) \quad (2)$$

where  $D$  is the horizontal divergence,  $E$  is the total deformation (stretching and shearing), and  $b$  represents the angle between the isentropes and axis of dilatation. An increase (decrease) in the gradient results in  $F > 0$  ( $F < 0$ ), and is said to be frontogenetic (frontolytic).

More recently, a vector frontogenesis equation was defined in a natural coordinate system with respect to the local orientation of the isentropes (Keyser *et al.* 1988):

$$\mathbf{F} = F_n \mathbf{n} + F_s \mathbf{s} \quad (3)$$

where  $\mathbf{F}$  is the vector frontogenesis function, and the quasi-horizontal contribution to the normal ( $\mathbf{n}$ ) and streamwise ( $\mathbf{s}$ ) components can be written as:

$$F_n = -\frac{D}{Dt} |\nabla_p \mathbf{q}| \quad (4a \text{ and } 4b)$$

$$F_s = \mathbf{n} \cdot (k \times \frac{D}{Dt} \nabla_p \mathbf{q})$$

The  $F_n$  component is the negative of (1) (measuring change in temperature gradient *magnitude*), while  $F_s$  measures the rate of rotation of the isentropes (temperature gradient *direction*). The vector frontogenesis function is fundamentally important to diagnosis of vertical motion in the atmosphere: it is Galilean invariant, and also represents a full wind generalization of the quasi-geostrophic (QG)  $\mathbf{Q}$ -vector (Keyser *et al.* 1988).

Observational experience suggests that the kinematics of the horizontal flow often play a dominant role in the field of both  $F_n$  and  $F_s$ . The component of frontogenesis normal to the isentropes is likely more focused on smaller spatial scales because it can be enhanced by convergence, largely a mesoscale process, whereas  $F_s$  is associated with vorticity and deformation which can be large on the synoptic-scale and associated with geostrophic motions. Since synoptic-scale divergence is small, deformation often initiates the banding process, with convergence increasing once thermal wind balance is disrupted and a secondary, ageostrophic circulation is established. Mesoscale bands are therefore well-approximated by horizontal deformation zones because they determine the approximate location of frontogenetic forcing that results in a narrow linear zone of ascending motion.

Idealized simulations by Keyser *et al.* (1988, 1992) demonstrate that  $F_n$  is associated dynamically with frontal-scale circulations, whereas  $F_s$  is associated with circulations on the scale of the synoptic disturbance.  $F_n$  (or simply  $F$ ) has proven to be a valuable diagnostic in forecasting mesoscale banding, particularly when vertical continuity of  $F_n$  is present through the 850-500mb layer. However, not all areas of  $F_n$  result in mesoscale banding, even in the presence of sufficient moisture for precipitation. There is cursory evidence to suggest that mesoscale bands are most robust not only when  $F_n$  is strong and well-defined through the 850-500 mb layer, *but also when it occurs spatially separate from the forcing associated with  $F_s$ .*

Let's assume in an absolute sense that a horizontal deformation zone exists and completely describes the kinematic field, and that the isotherms are oriented parallel to the axis of dilatation (Fig. 2), as is commonly observed.

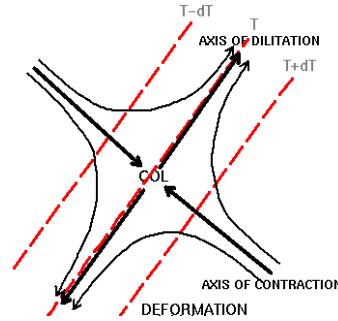


**Fig. 2** Kinematic motion described by pure deformation. The black lines represent streamlines. The dashed red lines represent isotherms. The COL label represents an area of zero velocity in the flow field.

As air parcels asymptotically approach the axis of dilatation, it is clear that there cannot be, in this special case, any kinematic contribution to the field of  $F_s$  at the level under consideration. However, the contribution to  $F_n$  can be quite large. This situation can result in robust mesoscale bands with little or no precipitation other than that associated with the bands, a situation that can result in extreme precipitation accumulation gradients.

Allowing for background translation, we would find that if the deformation zone is translating parallel to the axis of dilatation,  $F_s$  remains zero. Banding will likely be robust but perhaps shorter-lived locally as the deformation and frontogenesis move past. If the deformation zone is translating uniformly parallel to the axis of contraction, banding will likely again be robust ( $F_s=0$ ), however, the band will very quickly pass a given location. If the deformation zone is collocated with a horizontal shear zone, then  $F_s$  can be large and the organization of precipitation either will include bands embedded in a larger field of precipitation or will be non-banded in nature. The best scenario from a banding perspective would appear to be strong deformation (and convergence) with minimal translation or vorticity, such that a col point exists in a system-relative and an absolute sense, creating a very favorable environment not only for banding, but also for long-lived bands affecting one specific area.

We can consider local vertical wind profiles that observational experience suggests are conducive to different degrees of mesoscale banding (Fig. 3). Northeast of a strong cyclone, the mean vertical wind profile (Wc2) is characterized by strong warm advection

through a deep layer, and substantial (clockwise) turning of the hodograph (Bluestein and Banacos 2002) which, from the thermal wind relationship, suggests that the orientation of  $\nabla_p \mathbf{q}$  is changing with height.

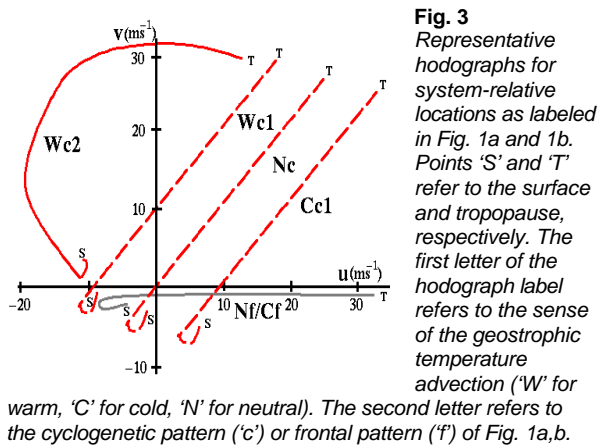


**Fig. 3** Representative hodographs for system-relative locations as labeled in Fig. 1a and 1b. Points 'S' and 'T' refer to the surface and tropopause, respectively. The first letter of the hodograph label refers to the sense of the geostrophic temperature advection ('W' for warm, 'C' for cold, 'N' for neutral). The second letter refers to the cyclogenetic pattern ('c' or frontal pattern ('f') of Fig. 1a,b.

Such an environment is generally not conducive for mesoscale bands, as the  $F_s$  contribution is generally strong and if  $F_n$  does exist, the plane of the circulation is not consistent with height, and no coherent banded structure will be observed. Precipitation is generally widespread, but not banded in this wind environment.

In the northwest quadrant of the cyclone, the hodograph structure tends to be straight, to a first approximation, with strong mid-level deformation as has been previously discussed. The Cc1 hodograph represents cold advection at the far edge of the cyclone's northwest sector. Some banding is possible, however, the tendency will be for precipitation to decrease in this region with time as cold advection decreasing with height leads to large-scale decent, consistent with the QG omega equation. In the case of Wc1, which is located east of the deformation zone, some banding is possible, but bands are generally short-lived features embedded within larger-scale precipitation associated with warm advection. In the case of Nc, the hodograph is straight and passes through the origin implying that the geostrophic temperature advection is zero. The col point aloft will often be a manifestation of a deformation zone, and may be associated with a local maximum in frontogenesis ( $F_n$ ) forcing. This should be a signal to the forecaster that the field of frontogenesis needs to be explicitly assessed, as very well-defined mesoscale banding is possible at this kinematic "sweet spot". The Nf/Cf hodograph represents an analogous situation where nearly calm winds occur within the important 850-500 mb layer, but for the frontal pattern (Fig. 1b).

#### 4. OBSERVATIONAL EXAMPLES

##### Case 1: Northern OR/eastern WA; 29 December 2002

As a mid-tropospheric phenomenon, mesoscale banding is not limited to areas east of the Rockies. During the early morning hours of 29 December 2002, an episode of mesoscale banding took place across northern Oregon and eastern Washington (Fig. 4a). The solitary band formed across north-central Oregon about

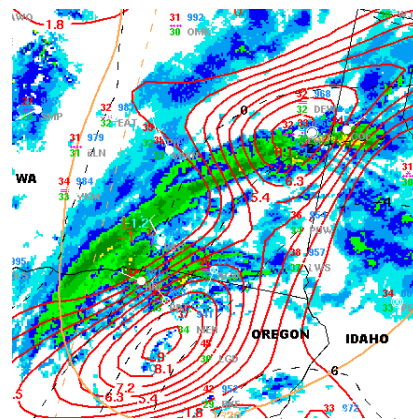


**Fig. 4a** Mosaic WSR 88D composite reflectivity at 0759 UTC on 29 December 2002. Red lines represent RUC 2h forecast frontogenesis at 850 mb valid at 08 UTC on the 29th.

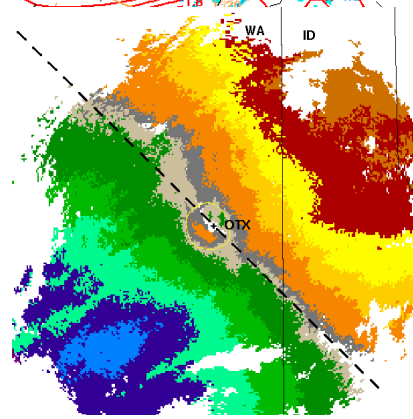


**Fig. 4b** Base velocity at 1.5° elevation from Spokane (OTX) valid 0854 UTC on 29 December 2002. Inbound motion is shown as shades of green and blue. Dashed line indicates area of zero radial velocity. Circle near radar denotes a level of zero velocity.

125 km west of Pendleton, Oregon around 5 UTC, in an area of pronounced 850 mb frontogenesis ( $F_n$  component unless otherwise noted). The reflectivity feature developed rapidly northeastward into south-central and eastern Washington, generally parallel to the deep-layer shear (Fig. 4b). The band intensified during the following 3-6 h, producing 1"/hr snowfall rates at Spokane (GEG) between 9-12 UTC.

A north-northwestward movement of an area of low-level warm advection preceded the formation of the band across far northeast Oregon, which resulted in a baroclinic zone moving over the primary interest region (not shown). Thereafter, an 850 mb low over north-central Oregon moved northeastward along the baroclinic zone, and along the axis of coincident deformation and convergence during the most intense period of banding. The band began to be shunted to the east around 12 UTC with the approach of a cold front and attendant upper trough axis from the west (not shown).

Particular attention is given to the structure of the wind field as depicted by the WSR-88D 1.5° base velocity image at 0854 UTC, the time at which heavy snow commenced over Spokane. It can be seen that the zero radial velocity line is relatively straight from northwest to southeast through the radar site, particularly near and to the southeast of the radar. The absence of turning winds with height suggests geostrophic temperature advection was minimal. Additionally, a zero-velocity "ring" is evident around the radar site at a height of 3-4 kft (Fig. 4b), suggesting a local stagnation/col point in the flow at that level. This is

close to where the maximum in frontogenesis forcing was found, in addition to the precipitation band itself (similar to hodograph Nc in Fig. 3). The structure of the wind suggests a local deformation zone acting frontogenetically, with an absence of isotherm turning in that region which likely minimized the  $F_s$  contribution to upward vertical motion, favoring a relatively narrow and isolated area of precipitation, as was observed.

### Case 2: Western ND/Montana; 21 October 2002

During the evening of 21 October 2002, a strong cold front and associated baroclinic zone was moving slowly southward through the northern Plains. Strong frontogenesis in the 750-650 mb layer (Figs. 5a,b) contributed to a linear axis of precipitation (Fig. 6) to the north of the surface cold front (not shown).

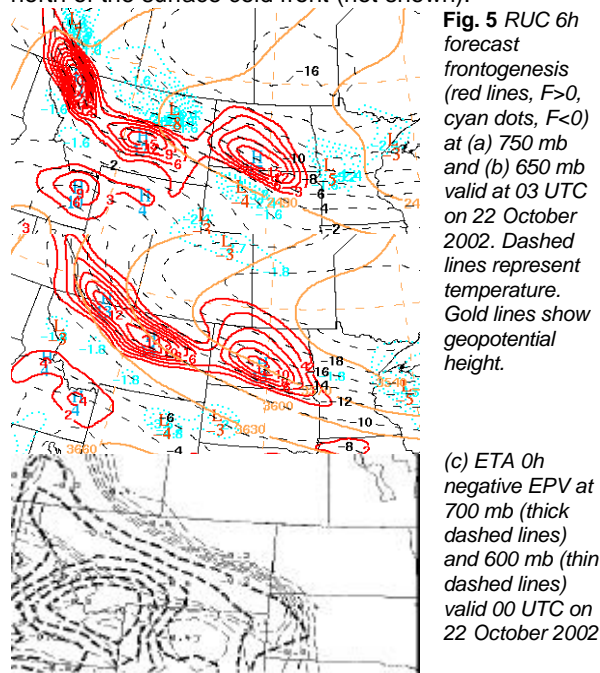


**Fig. 5** RUC 6h forecast frontogenesis (red lines,  $F > 0$ , cyan dots,  $F < 0$ ) at (a) 750 mb and (b) 650 mb valid at 03 UTC on 22 October 2002. Dashed lines represent temperature. Gold lines show geopotential height.

(c) ETA 0h negative EPV at 700 mb (thick dashed lines) and 600 mb (thin dashed lines) valid 00 UTC on 22 October 2002

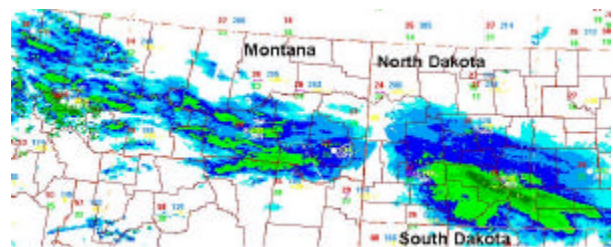


**Fig. 6** Mosaic WSR-88D composite reflectivity over the northern High Plains region at 0018 UTC on 22 October 2002.

Multiple banded structure was evident across much of Montana where equivalent potential vorticity (EPV) values (Moore and Lambert 1993) were negative (Fig. 5c), while a single band moved southward through the Bismarck area producing briefly heavy snowfall. Although no surface cyclone was associated with this band, it is noted that strong deep-layer shear and a weak flow region is evident in the Bismarck VAD wind profile at 2354 UTC (Fig. 7a). The hodograph (Fig. 7b) suggests slight low-level cold advection, consistent with

the southward motion of the band with time. In non-cyclogenetic cases, a mitigating factor in terms of prolonged heavy snow is the tendency for the mid-level baroclinic zone to move perpendicular to its long axis.

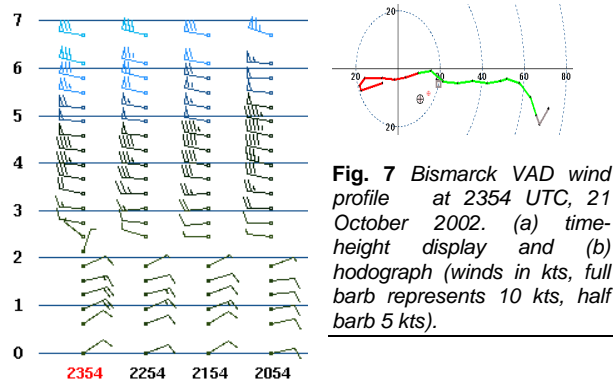


**Fig. 7** Bismarck VAD wind profile at 2354 UTC, 21 October 2002. (a) time-height display and (b) hodograph (winds in kts, full barb represents 10 kts, half barb 5 kts).

## 5. NUMERICAL MODEL CONSIDERATIONS

In the short-range (0-12 h), numerical model inadequacies in regard to the explicit prediction of upward vertical velocity (UVV) and mesoscale bands may stem from two primary factors. First, an initialization/data assimilation process that under-represents the beginning strength of a baroclinic zone in the low-mid troposphere, could result in "spin up" problems in regard to the ageostrophic circulation directly associated with the banding. Second, an undersampling of the mesoscale bands themselves (Barnes, 1994) is possible owing to inadequate horizontal grid resolution. The former problem can be diagnosed in areas with rawinsonde coverage or other observation data (ACARS, etc.) by comparing the initial 700 mb temperature distribution in the model to that of the observations. The potential for a stronger than forecast mesoscale band exists if the model-initialized baroclinicity is weaker than that suggested by nearby observations. This potential is heightened if the region is juxtaposed with forecast horizontal deformation or frontogenesis.

At longer time frames (beyond 12 h), forecast errors in cyclone track or frontal position guidance can significantly alter the position of 850-500 mb frontogenesis forcing. This limits predictability of the placement of such features, however, recognition of mesoscale banding potential over a general region is still possible based on the existence of frontogenesis and deformation. These forecast errors are analogous to forecasts of convective initiation, which is occasionally possible down to the county-scale at time < 6h, although the potential for convective initiation with strong synoptic-forcing is recognizable over a larger region at time-scales of several days. Utilization of numerical guidance must be done with considerable care at longer-time scales, where spatial errors can be significant, and at short-time scales where explicit development of mesoscale banding in terms of QPF and UVV cannot always be counted on even in the presence of well-defined model forecast frontogenesis. This attribute is shown in the next case example.

### Case 3: Southern New England; 7 February 2003

The “Blizzard of 1978” 25<sup>th</sup> anniversary snowstorm that affected southern New England on 7 February 2003 is used to illustrate a common deficiency in numerical guidance regarding prediction of banded precipitation, as well as the utility of explicit examination of the two-dimensional frontogenesis function ( $F$ ).

The snowfall accumulation map (Fig. 8a) for this system shows a relatively narrow axis of >12” extending from northern Rhode Island and south-central Massachusetts eastward to the coast, including Boston and points just to the south. Mosaic WSR-88D composite reflectivity data at 2010 UTC (Fig. 8b) across the region shows a distinct mesoscale precipitation band extending from eastern Long Island northeastward into Massachusetts Bay.

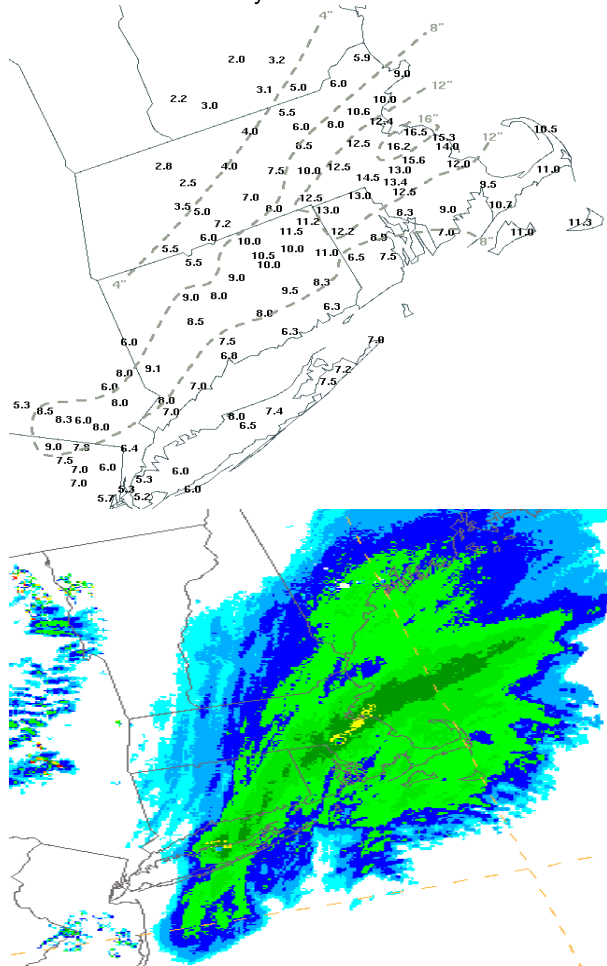


**Fig. 8** (a, top) Snowfall accumulations (inches) based on storm reports from NWS-WFOs Taunton, MA and Brookhaven, NY for the 7 February 2003 snowstorm. (b, bottom) Mosaic WSR-88D composite reflectivity at 2010 UTC, 7 February 2003. Yellow shading represents reflectivity values of 35-39 dBZ.

On the synoptic-scale, a surface cyclone deepened during the day as it moved rapidly from a position off the

Delmarva Peninsula at 12 UTC to several hundred kilometers east-southeast of Cape Cod by 00 UTC on the 8<sup>th</sup> (not shown). A closed low formed south of Long Island at 850 mb during this same period, however, the system remained an open wave at 700 mb. The pattern was somewhat atypical for the region as it reflected the positive tilt, open wave structure often seen in the northern Great Plains. The strong low-level baroclinicity on the northern edge of the Gulf Stream may have contributed to the deepening of the system at low-levels.

The band evolved in the following manner: between 14-15 UTC, an area of relatively high reflectivity developed across the lower Hudson Valley east-northeastward across northern Connecticut to an area just south of Boston. During the next 6 hours, the precipitation area appeared to contract while the mesoscale band intensified and became better defined (Fig. 9). The band rotated slowly counterclockwise around a pivot point centered near Norfolk County (in eastern Massachusetts), while the band itself moved eastward along its long axis. The band's forward speed and motion perpendicular to the long axis increased as it migrated offshore of southeastern Massachusetts between 21-00 UTC (not shown), as the surface low moved well east of the region and low-level cold advection increased across eastern New England.

The Rapid Update Cycle (RUC) model forecast from 09 UTC on the 7th is employed to examine this case from a model perspective owing to high temporal resolution and apparent accurate depiction of 2-D frontogenesis which was likely directly linked to band development and maintenance between 07/14-08/00 UTC. The field of 700 mb UVV at 15 UTC (Fig. 9a), 18 UTC (Fig. 9d), and 21 UTC (Fig. 9g) indicates a circular UVV maximum that remained generally offshore south and southeast of New England. Taken alone, the UVV and QPF patterns fail to adequately characterize the observed linear nature of the precipitation during the period of maximum snowfall intensity, and are in fact much more characteristic of the larger-scale geostrophic warm advection region at 700 mb which remained largely offshore (Fig 9c,f,i). However, the field of model 700 mb frontogenesis (Fig 9b,e,h) corresponded well with the linear band throughout its lifetime, suggesting that *it is advantageous to examine frontogenesis explicitly, irrespective of what the model UVV and/or QPF pattern may suggest.*

When viewed in the vertical, the field of 2-D frontogenesis corresponding to well-defined mesoscale banding, such as in this case, will frequently display a distinct “sloped continuity”, (Fig. 10) with the frontogenesis maximum displaced further into the colder air with height, indicative of a frontal structure aloft (which in extratropical cyclones is often unassociated with fronts at the ground). While the “sloped continuity” of the field is important to look for, either through assessment of several vertical levels or via cross-sectional means (Novak and Wiley 2002), it also raises the following question: given the sloped nature of the ascent, what vertical level most precisely represents

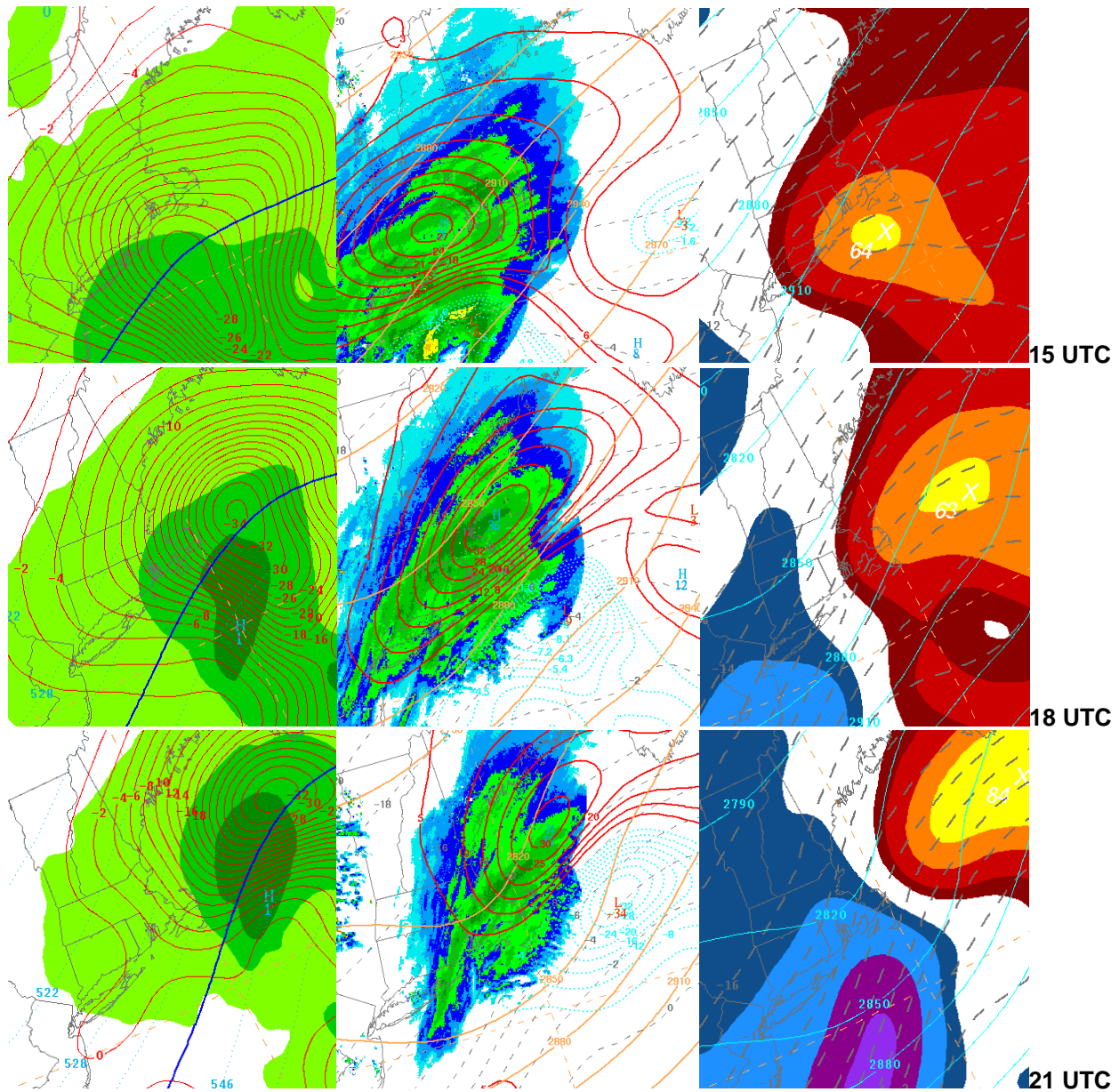


**Fig. 9** RUC model forecast panels valid at 15 UTC (top row, panels a,b, and c from L-R), 18 UTC (middle row, d,e,f), and 21 UTC (bottom row, g,h,i) on 7 February 2003. Left column displays model 700 mb UVV (solid contours, ub/s), 3 h accumulated precipitation (0.01", 0.25", 0.50" shading interval), and 1000-500 mb thickness (dotted lines, dm). Middle column shows mosaic WSR-88D composite reflectivity with 700 mb frontogenesis (solid red lines, positive; dotted blue lines, negative), 700 mb geopotential height (gold lines, m), and isotherms (dashed lines, °C). Right column displays 700 mb geopotential height and temperature (as in panels b,e,h) and 700 mb geostrophic temperature advection (shaded regions, yellow to red shades positive).

the spatial location of the associated banded precipitation?

Operational experience suggests the axis of maximum frontogenesis at 700 mb is perhaps most often aligned with the banded precipitation, however, it clearly can vary (e.g. around 850 mb in Case 1). It is often possible to improve upon the empirical "700 mb guideline" by searching for where there exists a col point in the flow aloft, either in observational data (very short-term) or model forecast soundings (longer-term), provided the model solution is reasonably accurate. In this case, the wind profiler at Plymouth, Massachusetts

(Fig. 11) indicates that during the time the snow band existed in a robust fashion over the area (15-21 UTC), calm/nearly calm winds were observed between 1-2 km AGL, suggesting the possibility of frontogenesis forcing even without looking at the diagnostic field. Prior to 15 UTC, low-level warm advection can be inferred at the site, followed by increasing cold advection after 21 UTC. Surface observations from Logan airport in Boston are shown in Table 1. The observations indicate that the period of maximum snowfall rates (1-2"/hr from 15-21 UTC) corresponded to the time the col point aloft was located nearby, with lesser rates before and after the col

existed locally. Thus, identification of the col point aloft may be able to assist in determining the frontogenetic level most closely associated with the time and place of mesoscale banding.

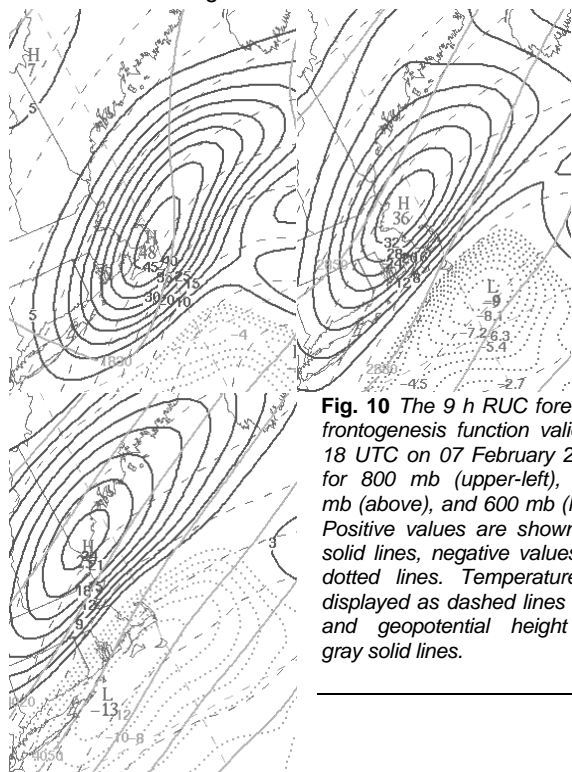


**Fig. 10** The 9 h RUC forecast frontogenesis function valid at 18 UTC on 07 February 2003 for 800 mb (upper-left), 700 mb (above), and 600 mb (left). Positive values are shown as solid lines, negative values as dotted lines. Temperature is displayed as dashed lines ( $^{\circ}\text{C}$ ) and geopotential height as gray solid lines.

**TABLE 1.** Surface visibility, precipitation, and hourly snow accumulation rate observations from Boston, Massachusetts (BOS), on 7-8 February 2003

BOS 13 UTC	1 1/2 SM	-SN
BOS 14 UTC	1/2 SM	SN
BOS 15 UTC	1/2 SM	SN SNINCR 1/ 2
BOS 16 UTC	1/2 SM	SN SNINCR 1/ 3
BOS 17 UTC	1/2 SM	SN SNINCR 2/ 4
BOS 18 UTC	1/4 SM +SN	SNINCR 2/ 6
BOS 19 UTC	1/4 SM +SN	SNINCR 2/ 8
BOS 20 UTC	1/4 SM +SN	SNINCR 2/10
BOS 21 UTC	1/4 SM	SN SNINCR 1/10
BOS 22 UTC	1/4 SM	-SN
BOS 23 UTC	2 SM	-SN
BOS 00 UTC	10 SM	

## 6. CONCLUDING REMARKS

At best, the existence of a col point somewhere in the 850-500 mb layer within a frontal zone or extratropical cyclone, where vertical shear and horizontal wind speeds are otherwise strong, will direct the forecaster to the location of a non-translating deformation zone, a location favorable for strong frontogenetic forcing and stagnant mesoscale forcing capable of producing heavy precipitation. It should be noted that col points aloft are not prerequisites or an assurance of mesoscale banding, or that heavy precipitation cannot occur through other means, only that their existence in baroclinic environments suggest a favorable aspect of the flow field appearing in a subset of banded events. When identified in model forecast

soundings, it can be utilized as a “signal” or “clue” that banding is possible, requiring further attention on the part of the forecaster (e.g. explicit examination of frontogenesis fields, monitoring of data from VADs, ACARS, profilers, etc., to see if later observations corroborate the model forecasts).

An increased emphasis on the importance of col points, and frontogenesis/deformation in general, seems warranted, especially given the ever-increasing demand for mesoscale detail in forecasts by the user community. Deformation has, over the years, been neglected in comparison to the attention given to vorticity and divergence in operational practice. There are renewed efforts within the NWS to train forecasters on aspects of mesoscale banding (e.g. Banacos 2002; Novak *et al.* 2002) given the emergence of new technologies to graphically convey mesoscale detail, and various misconceptions of the recent past (Schultz and Schumacher 1999).

The observational cases also demonstrate the need for a comprehensive climatology of banded precipitation in cases with and without cyclogenesis, with and without col points, and with or without the  $F_n$  forcing component in the vector frontogenesis equation. Observational work, to explicitly examine the mesoscale distribution of precipitation when  $F_n$  and  $F_s$  is juxtaposed versus spatially separated, would also likely be helpful to understand better the relationship between this partitioning of forcing and the nature of various precipitating systems.

## 7. ACKNOWLEDGMENTS

The author gratefully acknowledges Steve Weiss (SPC), Steve Corfidi (SPC), and Dr. David Schultz (NSSL/CIMMS) for their review of this paper.

## REFERENCES

- Banacos, P. C., 2002: *Frontogenesis forcing and banded precipitation*. NOAA/NWS/WDTB Winter Weather Workshop. Available online at: <http://www.wdtb.noaa.gov/workshop/WinterWxIII/index.html>
- Barnes, S. L., 1994: Applications of the Barnes Objective Analysis Scheme. Part I: Effects of Undersampling, Wave Position, and Station Randomness. *J. Atmos. Oceanic Technology*, **11**, 1433–1448.
- Bluestein H. B., and P. C. Banacos, 2002: The vertical profile of wind and temperature in cyclones and anticyclones over the eastern two-thirds of the United States: a climatology. *Mon. Wea. Rev.*, **130**, 477-506.
- Keyser, D., M. J. Reeder, and R. J. Reed, 1988: A generalization of Petterssen's frontogenesis function and its relation to the forcing of vertical motion. *Mon. Wea. Rev.*, **116**, 762-780.
- \_\_\_\_\_, B. D. Schmidt, and D. G. Duffy, 1992: Quasigeostrophic vertical motions diagnosed from along- and cross-isentrope components of the  $\mathbf{Q}$  vector. *Mon. Wea. Rev.*, **120**, 731-741.

Moore J. T., and T. E. Lambert, 1993: The use of equivalent potential vorticity to diagnose regions of conditional symmetric instability. *Wea. Forecasting*, **8**, 301-308.

Novak, D. R. and G. Wiley, 2002: Mesoscale snowband cross section. *Eastern Region AWIPS Tech. Note, No. 5.0-42.*, National Weather Service ER Headquarters, Bohemia, NY. 9 pp.

Novak, D. R., J. Waldstreicher, L. Bosart, and D. Keyser, 2002: *Anticipating mesoscale band formation in winter storms*. Available online at: <http://www.cira.colostate.edu/ramm/visit/banding.html>

Petterssen, S., 1936: Contribution to the theory of frontogenesis. *Geophys. Publ.*, **11**(6), 1-27.

Petterssen, S., 1940: *Weather Analysis and Forecasting*, McGraw Hill, 505 pp.

Schultz, D. M., and P. N. Schumacher, 1999: The use and misuse of conditional symmetric instability (CSI) as a diagnostic tool. *Mon. Wea. Rev.*, **127**, 2709-2732; Corrigendum, **128**, 1573.

Schultz, D. M., 2001: Reexamining the cold conveyor belt. *Mon. Wea. Rev.*, **129**, 2205-2225.

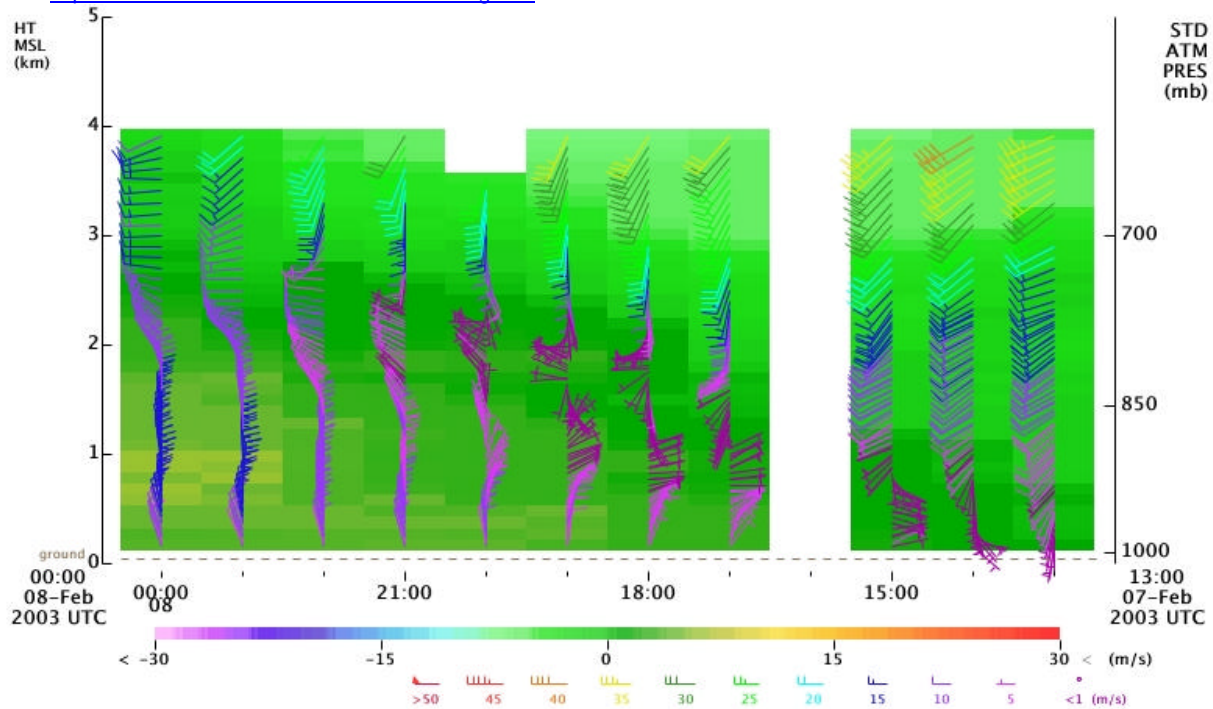


**Fig. 11** Time-height cross-section of the Plymouth, Massachusetts wind profiler directed 15 degrees north of vertical between 13 UTC 07 February, and 00 UTC 08 February 2003. Wind barbs represent hourly averaged horizontal wind, plotted in  $\text{ms}^{-1}$ . Shading represents hourly averaged radial (vertical) velocity in  $\text{ms}^{-1}$ .